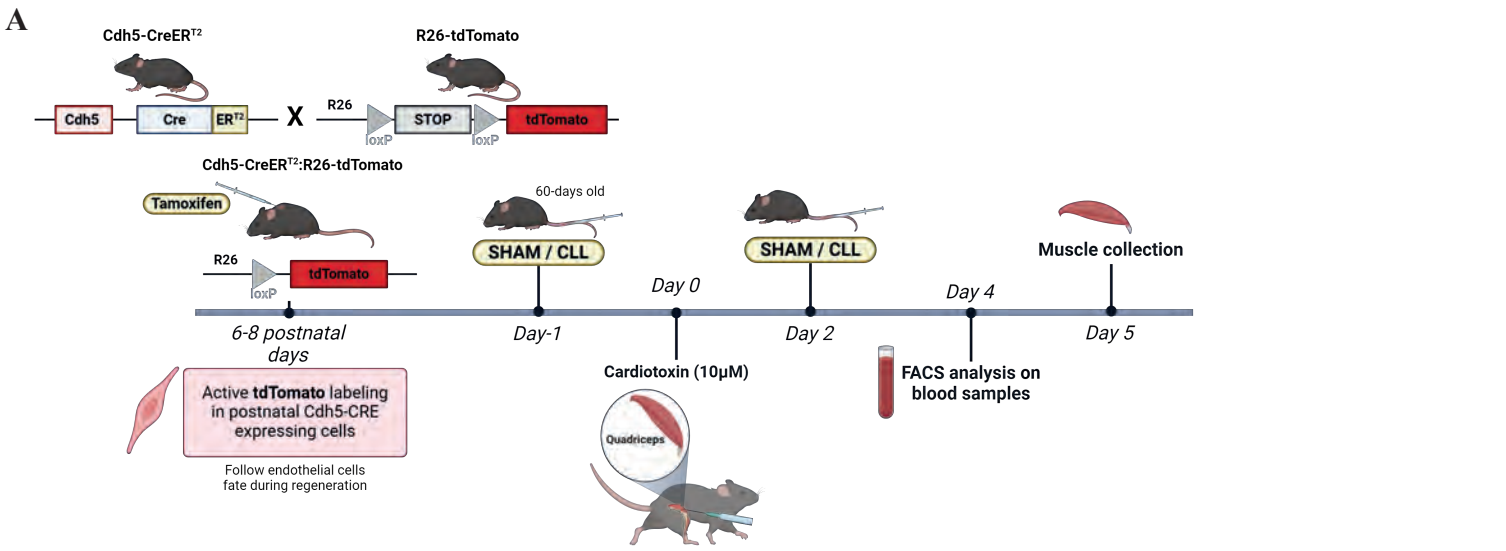

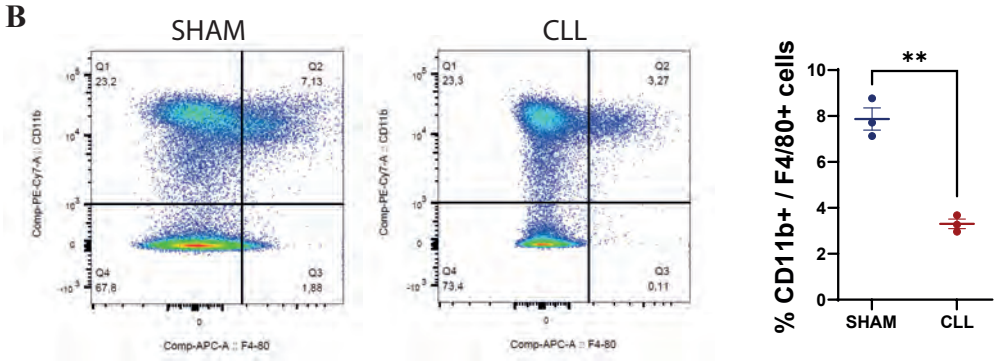

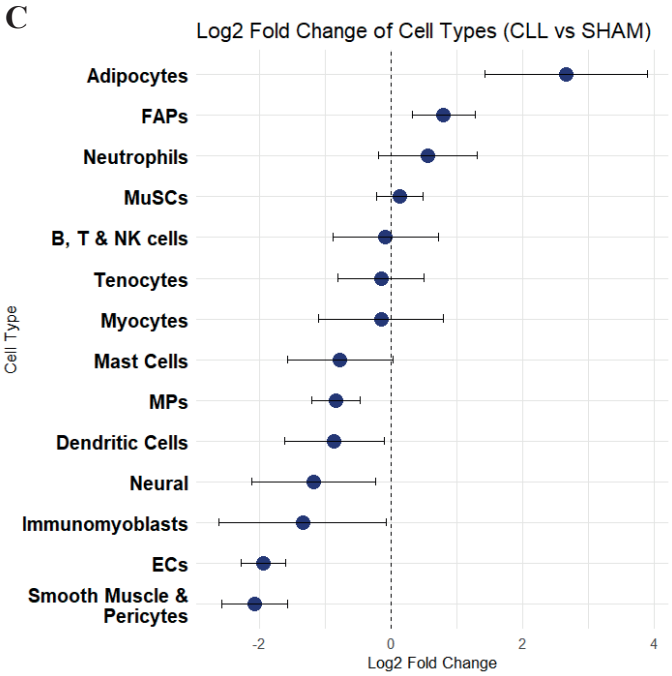

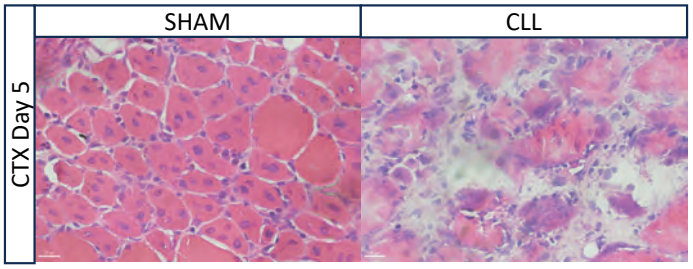

Supplementary Figure S1

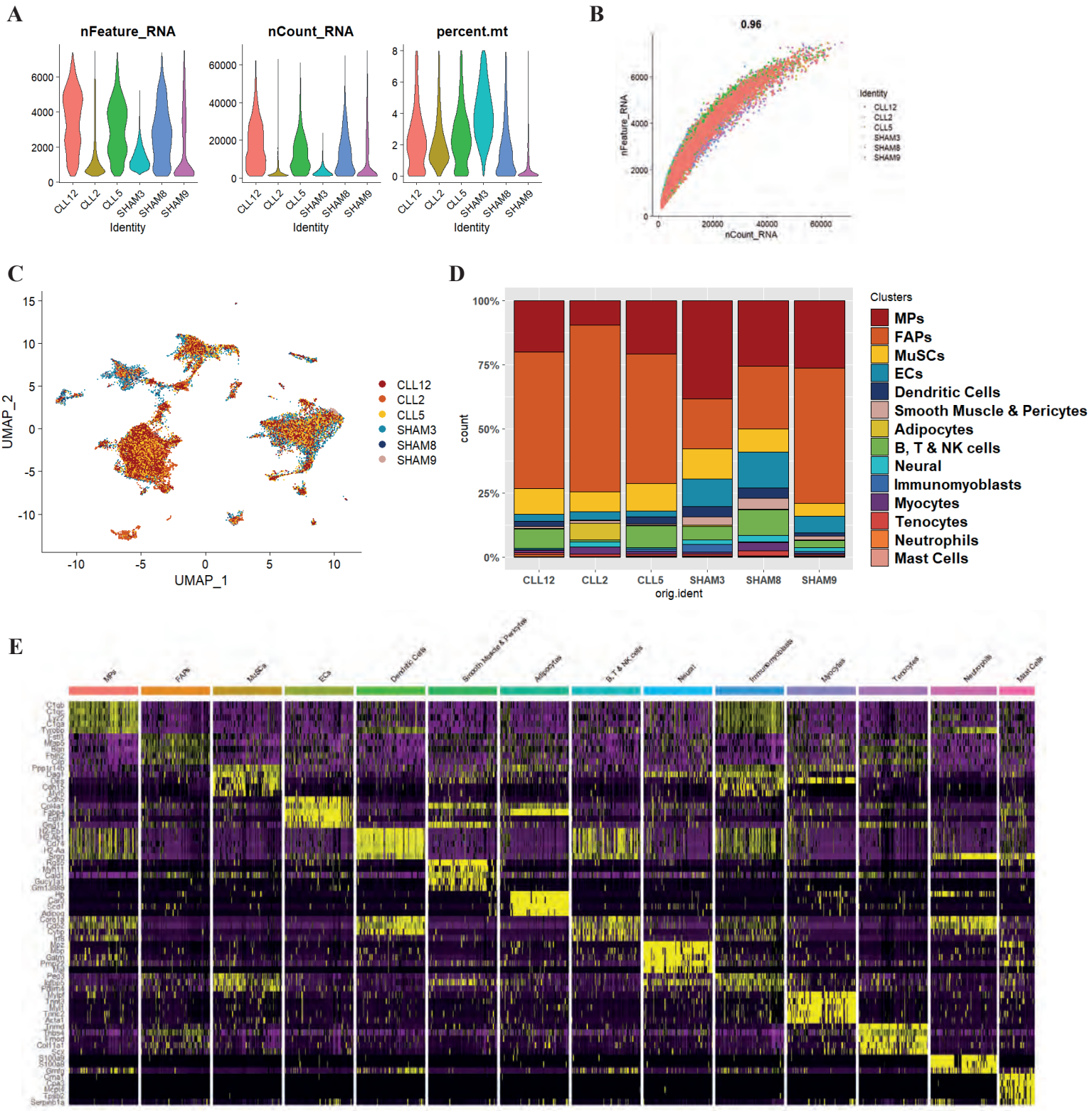

Supplementary Figure S2

A

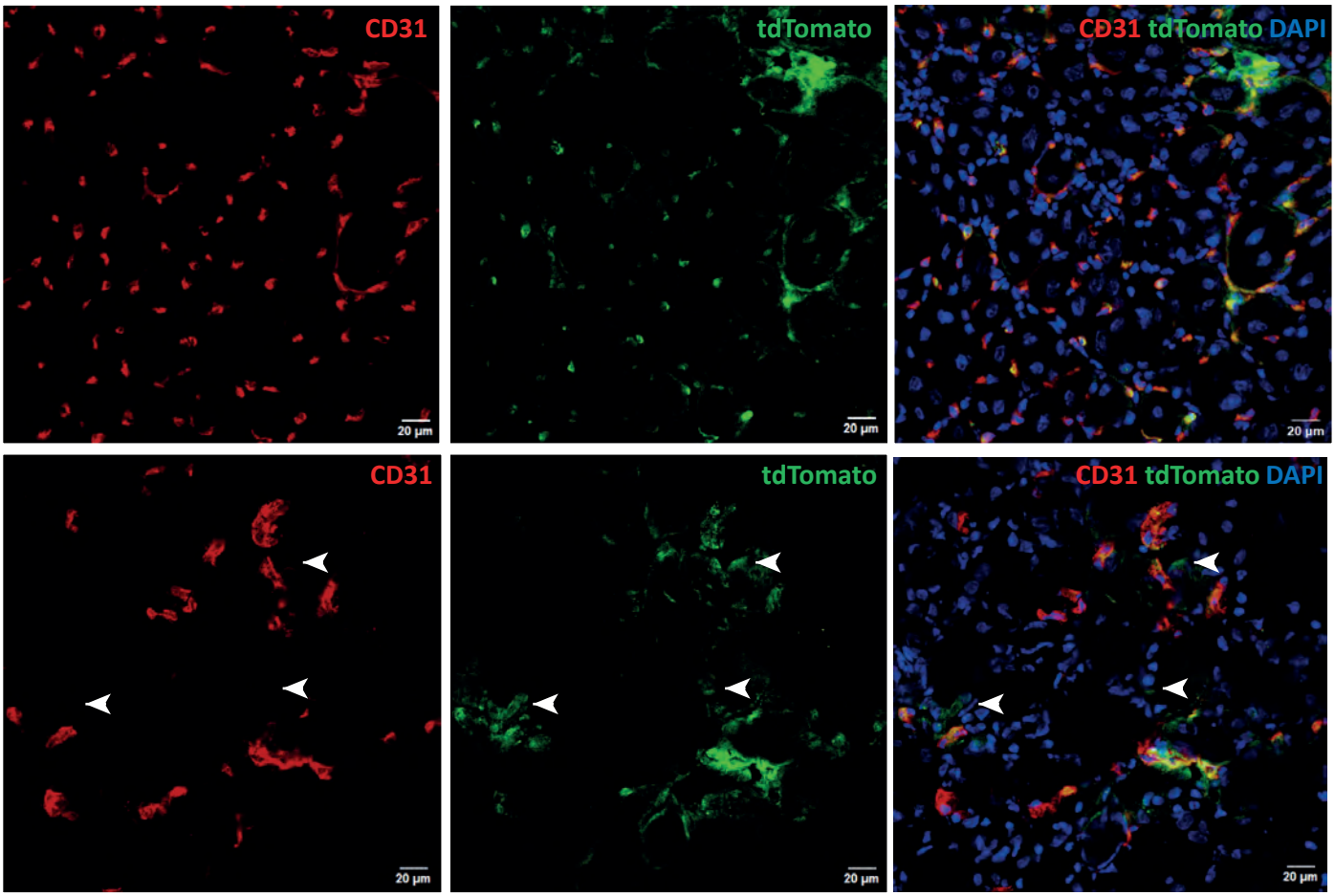

Supplementary Figure S3

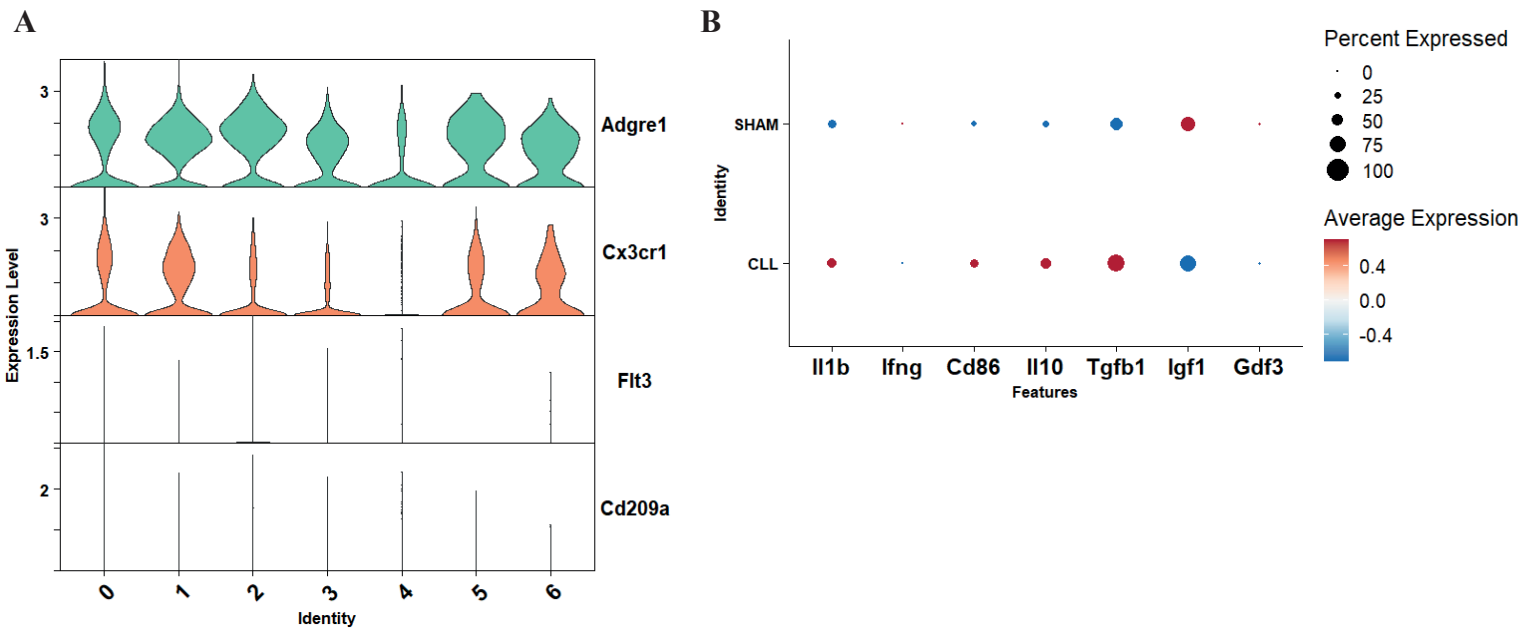

Supplementary Figure S4

A

	Source	Target	Ligand	Receptor	Prob	Pathway_name	Annotation	Evidence
SHAM	MPs	ECs	Gdf15	Tgfbr2	0,012	GDF	Secreted Signaling	KEGG: mmu04350
	MPs	ECs	Tnf	Tnfrsf1a	0,003	TNF	Secreted Signaling	KEGG: mmu04060

CLL	MPs	ECs	Gdf15	Tgfbr2	0,007	GDF	Secreted Signaling	KEGG: mmu04350
	MPs	ECs	Tnf	Tnfrsf1a	0,010	TNF	Secreted Signaling	KEGG: mmu04060
	MPs	ECs	Spp1	Cd44	0,019	SPP1	Secreted Signaling	PMID: 21907263
	MPs	ECs	Spp1	ITGAV_ITGB1	0,031	SPP1	Secreted Signaling	PMID: 21907263
	MPs	ECs	Spp1	ITGAV_ITGB5	0,011	SPP1	Secreted Signaling	PMID: 21907263
	MPs	ECs	Spp1	ITGA5_ITGB1	0,035	SPP1	Secreted Signaling	PMID: 21907263

B

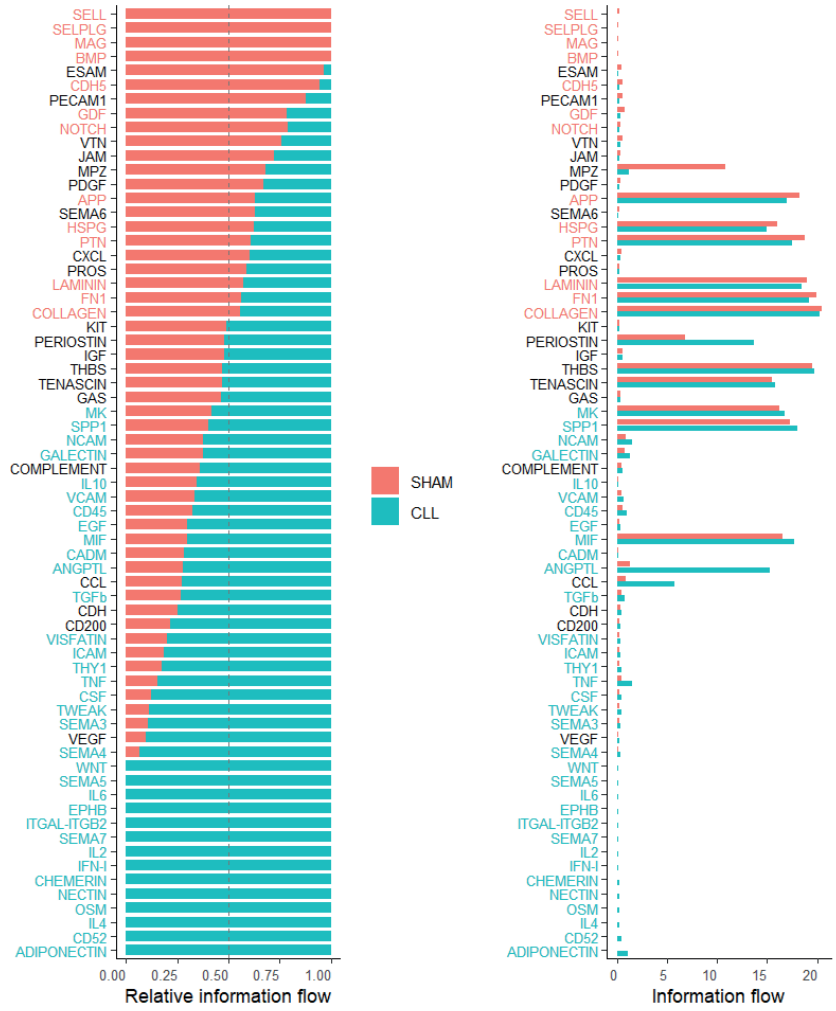

C

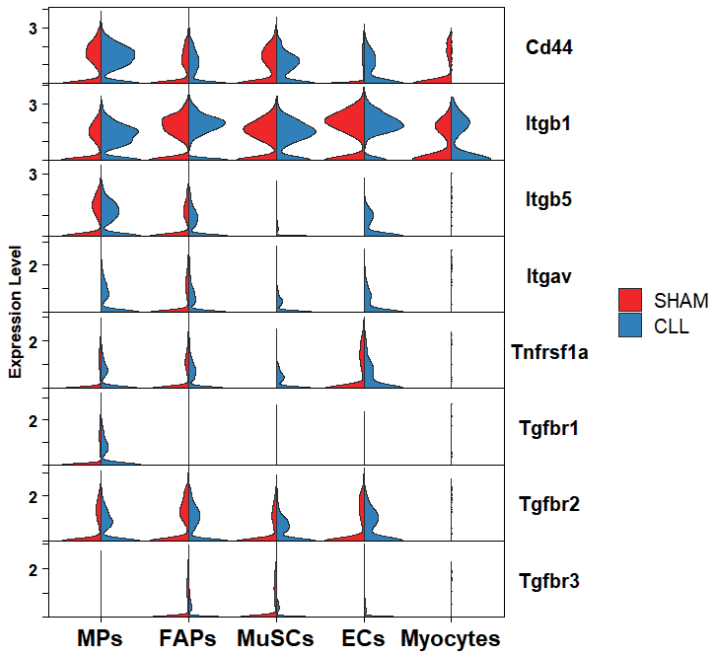

Supplementary Figure S5

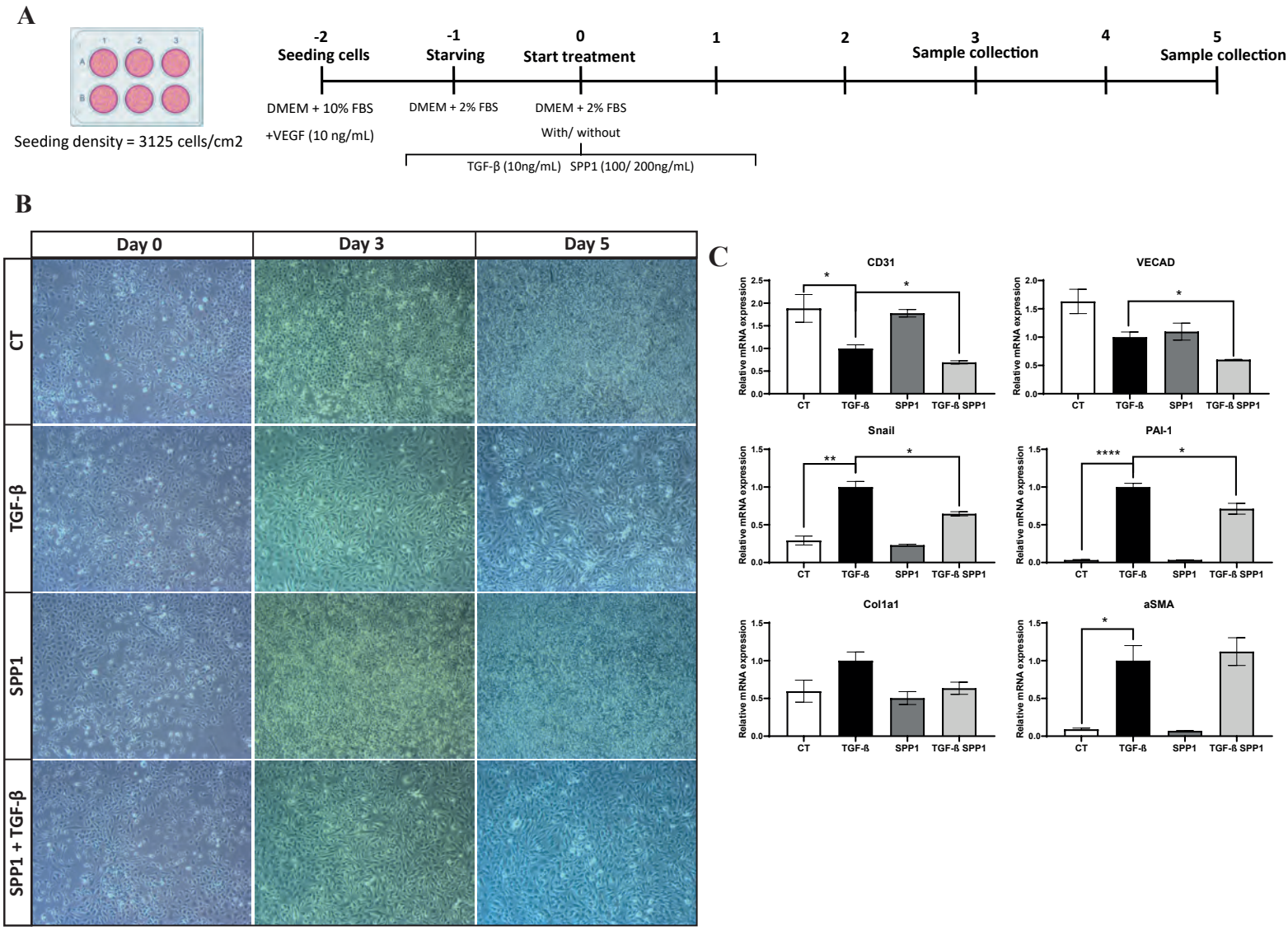

Supplementary Figure S6

Supplementary Figure Legends

Figure S1. Related to Figure 1: EndMT experimental setup

(A) Experimental scheme of EndMT triggering. Cdh5-CreERT2:R26R-tdTomato mice were equally divided in two groups and intravenously (IV) injected with liposomes containing Clodronate (CLL) or PBS as control (SHAM), one day before and two days after acute muscle damage induction by Cardiotoxin (CTX) on quadriceps.

(B) Gating strategy and percentage of Cd11b+ and F4/80+ cells (monocytes) in the blood of CLL vs. SHAM treated mice, 4 days after injury. Data is presented as mean ± SEM (n=3). Statistically significant difference is indicated as ∗∗ and represents $P < 0.01$ (two-tailed unpaired Student's t-test).

(C) Log2FC of the different cell types in CLL relative to SHAM. Each point represents the mean log2FC of cell proportions across replicates, with error bars indicating the standard error of the mean (SEM).

(D) H&E staining of quadriceps muscle cross-sections of SHAM- and CLL-treated Cdh5-CreERT2:R26R-tdTomato mice 5 days post cardiotoxin injury. Magnification 40x, Scale bar at 20 μm.

Figure S2. Related to Figure 1: Technical and quality control measures for scRNA-seq datasets and their analysis.

(A) Violin plots of all sequenced samples showing the distribution of the number of genes (nFeature_RNA), number of RNA counts (nCount_RNA) and percent mitochondrial RNA (percent.mt) after quality control filtering.

(B) The number of genes and RNA counts detected in each droplet, after quality control filtering for each sample.

(C) Integration of all sample replicates and their UMAP embedding coloured by sample.

(D) Relative cell proportions between sequenced samples.

(E) Heatmap of the top 5 expressed genes for each cell cluster. FindAllmarkers function was performed on Seurat 4.3.0.1 using non-parametric Wilcoxon rank sum test with parameters min.pct = 0.01, thresh.use = 0.1, only.positive = False and return.thresh = 0.01, to find all markers for each cluster.

Figure S3. Related to Figure 3: ECs undergoing EndMT

(A) Immunofluorescence staining of quadriceps muscle cross-sections of SHAM- and CLL-treated Cdh5-CreERT2:R26R-tdTomato mice 5 days post cardiotoxin injury for ECs (CD31, red), tdTomato (green) and nuclear marker (DAPI, blue). White arrows indicate examples of ECs that underwent EndMT (CD31-/tdTomato+ cells). Magnification 40x, Scale bar at 20 μm.

Figure S4. Related to Figure 4: Macrophage subpopulations characterization

(A) Violin Plot showing normalized and log-transformed expression of representative MP and dendritic cell specific markers on MP subpopulations

(B) Relative proportion and frequency of MP subtypes per condition.

(C) DotPlot demonstrating expression of pro-inflammatory and anti-inflammatory representative genes. Dot size indicates the percentage of cells expressing each gene, and dot colour represents the average expression level.

Figure S5. Related to Figure 5: Macrophage and Endothelial cell interactions

(A) Results table highlighting the difference in communication probability dependent on Gdf15, Tnf and SPP1.

(B) Bar chart of the significantly enriched pathways of SHAM and CLL mice. Pathways coloured in red are significantly enriched in SHAM, and pathways coloured in blue are significantly enriched in CLL mice.

(C) Violin Plot showing the expression of Spp1, Tnf and TGF-β receptors on MPs, FAPs, MuSCs and ECs populations between conditions.

Figure S6. Related to Figure 6: In vitro study of EndMT and SPP1 effect

(A) Experimental scheme of EndMT induction in vitro.

(B) mECs at day 0, 3 and 5, in the different experimental conditions: Control (CT), TGF-β, SPP1, and SPP1+TGF-β

(C) Relative gene expression levels of endothelial and mesenchymal markers of CT, TGF-β, SPP1, SPP1+TGF-β treated mECs. Results are normalized to GAPDH. Data is presented as mean ± SEM (n=3). Statistically significant differences are indicated as ∗, ∗∗, ∗∗∗ and ∗∗∗∗ representing $P < 0.05$, $P < 0.01$, $P < 0.001$ and $P < 0.0001$, respectively (two-tailed unpaired Student's t-test).